JOURNAL OF MATERIALS SCIENCE 17 (1982) 2199–2207

Fractographic studies of microstructural development in hydrated Portland cement

B. J. DALGLEISH, P. L. PRATT,
Department of Metallurgy and Materials Science, Imperial College of Science and Technology, Prince Consort Road, London SW7 2BP, UK

E. TOULSON
JEOL (UK) Ltd, JEOL House, Grove Park, Colindale, London NW9, UK

A comprehensive study of early hydration and morphological development in freeze-dried Portland cement paste has been carried out using scanning electron microscopy in conjunction with energy dispersive X-ray analysis. The microstructure develops from its early appearance as a porous C–S–H spherulite structure containing hexagonal CH crystals, with Hadley grains and large inherent pores being significant features, to one of large CH dispersions in massive C–S–H. Some aspects of microstructural influence on mechanical properties are discussed.

1. Introduction

Tricalcium silicate (C_3S)*, dicalcium silicate (β-C_2S), tricalcium aluminate (C_3A), and calcium aluminoferrite of variable composition (C_4AF) are the major components of anhydrous Portland cement. The compounds react with water to yield a paste that sets and eventually hardens to a porous composite of numerous hydration products that are morphologically distinct.

The reaction mechanisms that occur during the hydration process are not clearly understood: these include in particular the existence of an induction period and its termination after the first few hours. Current theories offer conflicting explanations which cannot be resolved without more detailed observation of the formation of the microstructure during the early stages of hydration. Furthermore, the chemical and morphological characterization of early hydration products, and their structural development as the paste matures, is essential to an interpretation of the relationship between the microstructure and mechanical properties in material hydrated in bulk. An understanding of the ways in which the microstructure can determine fracture behaviour may suggest ways of improving the strength. Scanning electron microscopy (SEM), used in conjunction with energy dispersive X-ray analysis, has proved particularly useful in such studies, and Diamond [1] has suggested a systematic nomenclature for the C–S–H gel structure, and named four distinct types of morphology (Types I to IV). Of these, Types I and III are found in our work, Type I being a fibrous morphology and Type III consisting of small irregularly equant or flattened particles. SEM reveals a three-dimensional structure organization, especially in young pastes, which aids the interpretation of images observed in transmission electron microscopy (TEM) [2], and thus should assist the identification of the microstructural flaws which determine the strength and fracture toughness of the material.

A mature cement paste consists of massive

*Cement chemists use a shortened notation: C = CaO; S = SiO_2; A = Al_2O_3; $\bar{S}$ = SO_4; F = Fe_2O_3; H = H_2O; C_3S = $3CaO \cdot SiO_2$; C–S–H = calcium silicate hydrate.

0022–2461/82/082199–09$03.58/0

Portlandite (CH) and calcium silicate hydrate of variable composition (C–S–H) which between them comprise up to 85% of the hydrated structure. The "AFt" phase related to the trisulphate, ettringite ($C_3A \cdot 3C\bar{S} \cdot H_{32}$) and the "AFm" phase related to monosulphate ($C_3A \cdot C\bar{S} \cdot H_{12}$) are present in small amounts, and a few unhydrated cores are observed. Most of the porosity is very fine and associated with the C–S–H gel structure, but a significant proportion is present as large flaws. The extent to which the various microstructural features determine mechanical properties continues to be the subject of much debate [3, 4].

2. Experimental method

The oxide analysis and Bogue composition of the Northfleet OPC used in this study are given in Table I. The development of microstructure in bulk cement paste hydrated for periods of up to 8 months has been investigated by examining "freeze-dried" samples prepared from the same mix. Paste was mixed using a distilled water/cement ratio of 0.5, cast and allowed to set in sealed polythene moulds. All variables except the degree of hydration were held constant. Samples hydrated for more than 24 h were demoulded after this time and cured under lime-saturated water until required for freeze-drying as previously described [2].

Cement paste develops very little cohesion in the first few hours of hydration so that samples hydrated for less than 10 h collapsed to powder during freeze-drying. These powder samples were examined as thin particulate layers, dispersed on specimen stubs using double-sided adhesive tape.

The powder specimens and fracture surfaces were prepared from bulk hydrated samples, and coated with gold just prior to examination in a JEOL JXA 35 system. Gold coating (about 10.0 nm layer) was used in preference to carbon to take advantage of the improved resolution of the image, even though gold interferes with sulphate analysis. (The main $\bar{S}$ lines fall within the wavelength range of the AuMα_1 peak at 2.123 keV).

TABLE I Analysis of Northfleet OPC clinker

Oxide	Analysis (%)	Bogue	Composition (%)
CaO	64.7	C_3S	54.5
SiO_2	20.8	C_2S	18.5
Al_2O_3	4.8	C_3A	8.9
Fe_2O_3	2.2	C_4AF	6.9
MgO	1.08		
Na_2O	0.2		
K_2O	0.5		
SO_3	2.8		
Free CaO	1.8		

3. Results and discussion

The X-ray analyses referred to were qualitative because of the normal problems of electron-beam penetration and spreading, absorption and fluorescence effects due to high points on rough fracture surfaces and, finally, difficulties in obtaining well-characterized standards. Nevertheless, the analyses serve to indicate the chemical nature of the morphologies observed.

3.1. Microstructure of clinker

A typical bulk clinker contains crystals of C_3S and β-C_2S embedded in a fine-grained matrix of phases such as C_3A and variable composition aluminoferrite (C_4AF). The C_3S crystals are about 50 μm in size and angular in shape whilst the β-C_2S crystals are smaller and often spherical. When the clinker is ground some of the particles may be monomineralic, but the majority are likely to be composites.

Fig. 1a shows a dispersed sample of as-received Northfleet OPC, the larger particles of which display the angularity and spherical nature expected for C_3S and β-C_2S, respectively. The largest particle approaches 70 μm in size and a number of others approach 30 μm. We have carried out particle-size analysis, using Coulter counting, which revealed up to 30% vol of particles greater than 30 μm, and up to 3% vol of particles greater than 90 μm. At higher magnification (Fig. 1b), some isolated pores and channels were observed on the surfaces of the large particles, but there was no evidence of an inter-connected system of microporosity.

X-ray analysis of the larger particles revealed Ca/Si ratios consistent with C_3S and β-C_2S, and included traces of Al, $\bar{S}$, K and Fe. Increased Al, $\bar{S}$ and Fe contents associated with the fine particles of Fig. 1a were consistent with Al and Fe being contained in the fine-grained matrix phases of the bulk clinker, and with gypsum which is relatively soft compared with the clinker phases, being more finely ground. (Gypsum, $CaSO_4 \cdot 2H_2O$, is ground with the bulk clinker, and is added to retard the normally rapid hydration of C_3A). Separation of Northfleet OPC into particle-size fractions, and subsequent X-ray fluorescence analysis, confirmed these findings.

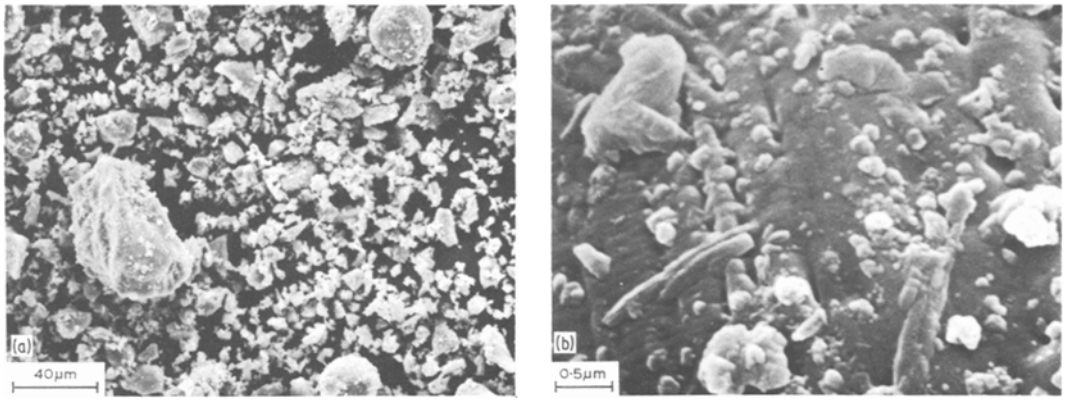

Figure 1 (a) Dispersed particles of as-received cement powder. (b) Surface of particle of as-received cement powder.

3.2. Kinetics of hydration

The hydration reaction is best followed by monitoring the rate of heat evolution as a function of time, using an isothermal calorimeter. The calorimetry curve of a cement typical of that used in this study is shown in Fig. 2. A short initial burst of reaction, Stage I, is followed by a few hours of relative inactivity, Stage II, but very small amounts of "early product" are observed to form throughout this induction period. The reaction then proceeds rapidly as "middle product" forms in Stages III and IV, whereupon it slows to a more or less constant rate with the formation of "late product" during Stage V. The shoulder on the main heat evolution peak is very often associated with the conversion of C_3A and C_4AF to monosulphate, but some microstructural evidence [5] suggests an association with the large-scale formation of ettringite.

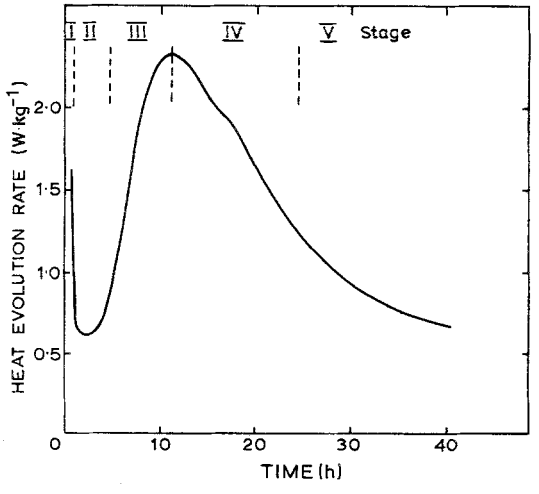

Figure 2 Heat evolution during hydration of cement.

The early reaction sequence of this particular cement has been discussed previously [5]. The rate of reaction and heat evolution is very similar to that observed for a wide variety of cements. However, the details of structural development are typical of only some of the cements that we have observed.

3.3. Development of products of hydration

3.3.1. Early product

After 1 h (Fig. 3) the initial burst of hydration is seen to have produced a textural change of the surfaces of the cement particles due to the formation of a discontinuous layer of angular rod-like product some 0.25 μm long and 0.1 μm thick, typical of "AFt" growth.

The textured surfaces of cement particles can be observed at lower magnification in Fig. 4 which shows a sample of dispersed two-hour paste. Coarse crystal platelets and rods are also present in significant proportion, superimposed on the structure of Fig. 3, and X-ray analysis indicated

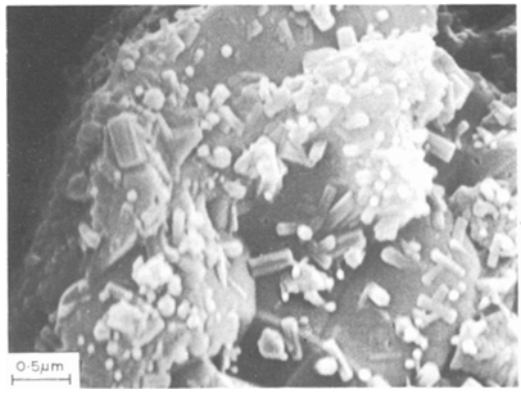

Figure 3 Surface of particle after 1 h hydration.

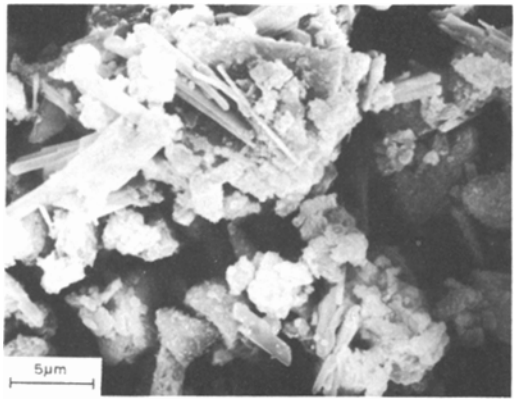

Figure 4 Dispersed particles after 2 h hydration.

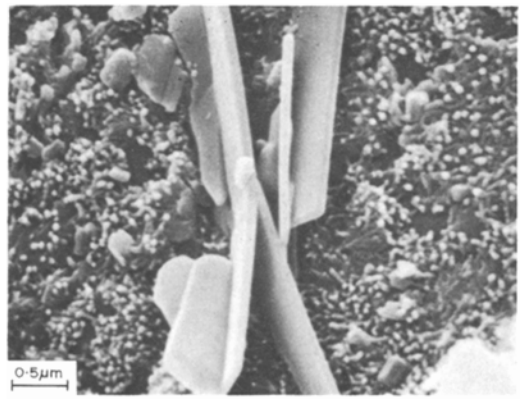

Figure 5 C–S–H nucleation and CH precipitation on the surface of a dispersed particle of four-hour cement paste.

that this coarse material was gypsum. This is expected to dissolve rapidly in water during the initial mixing, and appears to have recrystallized during freeze-drying.

3.3.2. Middle product

For the Northfleet OPC used in this study, four hours hydration brings the induction period to an end as C–S–H starts to nucleate and CH precipitates as thin platelets. The suggested mechanisms governing the induction period and its termination are presently the subject of much discussion, and are centred around two main theories. The first theory attributes the induction period to delayed nucleation of CH and/or C–S–H [6], the period ending when nucleation commences. In the second theory the induction period commences with the formation of a protective surface layer on the cement particles, and ends when the layer is disrupted [7, 8]. Double *et al.* [7] believe this occurs when sufficient osmotic pressure is generated. On the other hand, Jennings and Pratt [8] have suggested that CH precipitation first weakens and finally ruptures the protective membrane either by heat and/or mechanical stress associated with the formation of CH. Whether precipitation first occurs on the inside or the outside of the membrane is not clear, but it does so near the surface. Fig. 5 shows CH precipitation on the surface of a particle hydrated for four hours.

Particles of dispersed six-hour paste are shown in Fig. 6a, and the central particle has a coarse surface texture compared with that of the particles on either side. At higher magnification (Fig. 6b) the coarse texture is seen to be composed of the short hexagonal rods associated with "AFt" growth from C_3A and C_4AF. X-ray analysis of the features shown in Fig. 6b revealed high Al, $\overline{S}$ and Fe contents, which is consistent with the view that significant substitution of Fe for Al can occur in the formation of the calcium aluminate sulphate hydrates [1]. The size of the central particle in Fig. 6a, about 9 μm, is larger than expected for C_3A or C_4AF, and probably represents either hydration of a polymineralic fragment of clinker matrix, or hydration of a matrix layer existing on a C_3S or β-C_2S grain.

Continued hydration results in the cement becoming coated with a layer of product in the form of fibres radiating out from the unhydrated cores, and in the formation of Hadley grains. Fig. 7 shows the increased fibrous development of C–S–H after 18 hours hydration, with some fibre overlap between adjacent particles, and two Hadley grains in the central region. The contribution of this fibrous structure with regard to paste properties, and more importantly the question of whether it is an artifact of drying, have been discussed [8]. Clearly, the influence of rapid drying techniques on the observed microstructure, particularly of young pastes, needs to be established.

Figs 8a and b show two examples of the Hadley grain, a relatively new feature of the cement paste microstructure observed in the SEM [9] at higher magnification. During fracture the hydration layer, about 1 μm in thickness, has been broken to reveal a partially hollow shell containing an unhydrated core, with some of the interior space bridged by rods. Hadley grains were a common feature of the fracture surfaces examined in this study.

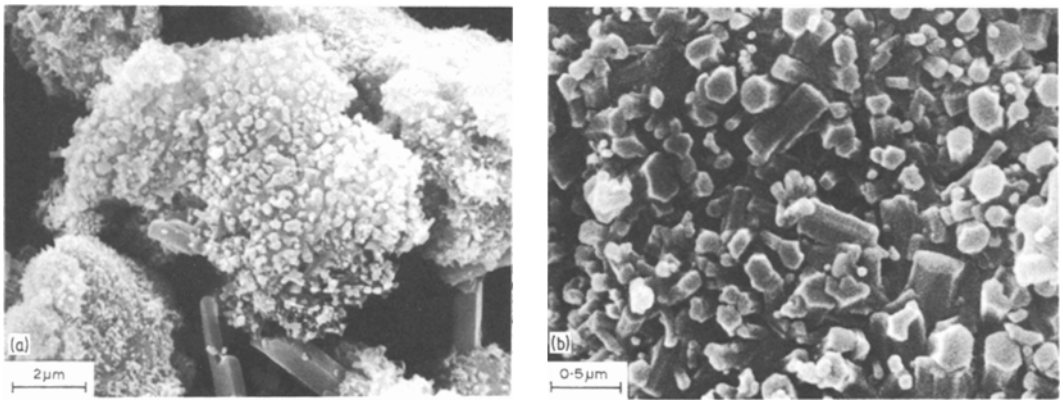

Figure 6(a) The variation in surface morphology of some dispersed particles of six-hour cement paste. (b) The central coarse-textured grain of (a) at higher magnification.

The mode of hydration in Hadley grain formation would appear to be one in which a thin layer of early hydration product forms on the grain surface, and the grain is then subjected to dissolution from within the shell to produce either a completely hollow shell or one which is partially hollow and contains a remnant cement grain. An example of the latter is shown in Fig. 8a, in paste hydrated for one day; a single-point X-ray analysis suggests that the remnant grain is calcium silicate in this case. The surface of the remnant grain has a dimpled texture which may be the result of etching. The initial hydration layer is composed mainly of short rods typical of "AFt" growth, and both the layer thickness and width of interior space approach 1 μm. Some of the rods are longer and bridge the interior space and protude through the shell, while others are attached to the surface of the unhydrated core (Fig. 8b). There is some evidence of hollow "AFt", which could be a means whereby solution was expelled from the confines of the shell into surrounding space. However, in addition, SEM studies of polished and etched surfaces of young cement paste [2] have shown cracks bridging hydration layers, and certainly the rate of hydration in Stages III and IV is rapid.

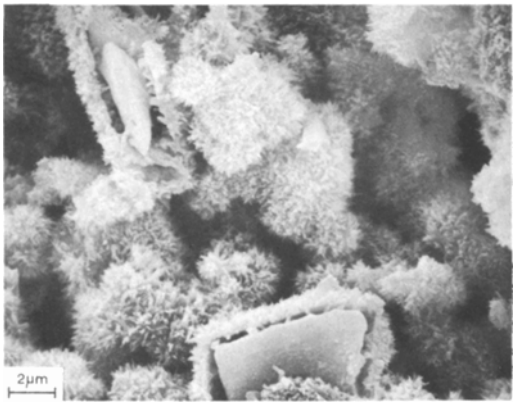

Figure 7 Developing C–S–H structure (Type I) in an 18-hour paste, showing examples of Hadley grains.

It has been argued that the hollow shell features are the result of the rapid drying of young pastes, but current SEM studies of pure freeze-dried C_3S have shown a notable absence of such hydration features. Also Barnes *et al.* [9] observed Hadley grains in all ages of paste up to 28 days, and we have observed them after 2 months hydration.

Thus the present work is in agreement with Barnes *et al.* [9] and with our preliminary thin-foil studies [10] that Hadley grains are a significant feature of the hydrated cement paste microstructure. Since porosity develops as a result of their formation, further characterization of the hollow shells is required, especially of their contribution to the properties of mature paste. The size of the pores generated is necessarily fairly large because small cement grains rapidly undergo complete hydration. Also, because Hadley grains are numerous and dispersed throughout the micro structure, the distribution of general porosity will be important. Understanding the influence of pore size and shape, and the distribution of total porosity, on the mechanical properties of Portland cement may lead to improvements in the strength and Young's modulus of the material.

3.3.3. Late product

The fracture surface of a three-day cement paste

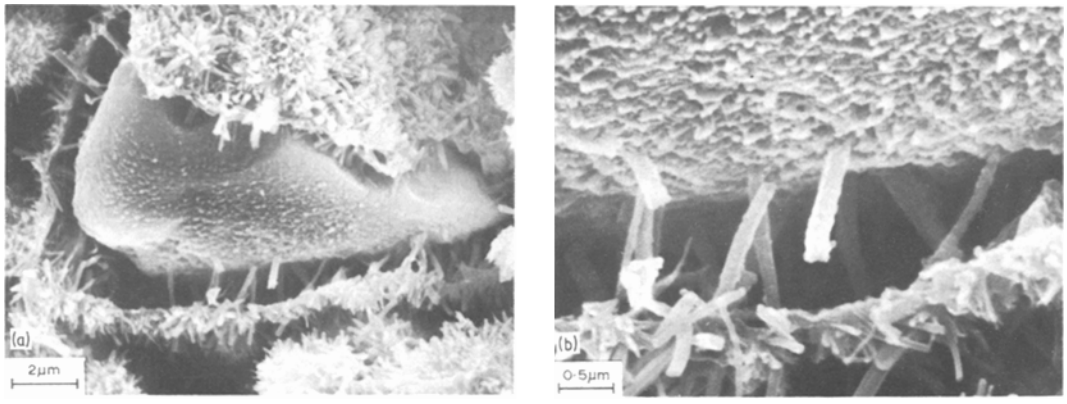

Figure 8(a) A Hadley grain in one-day cement paste. (b) The hydration shell morphology and core texture of (a) at higher magnification.

is shown in Fig. 9. A large amount of interparticle porosity is evident, and the hydrating grains are enmeshed in an interconnected framework of fibres. At this stage CH has changed from its early appearance as thin plates, and has grown into the space between the cement particles as large crystals which engulf other constituents. X-ray analysis of CH crystals often contain contributions from entrapped species [11]. At higher magnification (Fig. 10) some of the fibres are seen to be morphologically similar to "AFt" and X-ray analysis revealed significant Al, $\overline{S}$ and Fe counts. Some of these fibres have a uniform cross-section along their length, with flat ends, and display a "floral" section. Similar features have been observed during *in situ* studies in transmission at high voltage [12].

Another newly observed, but common, feature of the cement paste microstructure, initially found during STEM examination [2], is the appearance of a series of spherulites of C–S–H. They are readily observed on the fracture surface of cement specimens from one day up to about 20 days old. The majority are very small, about 3 μm in diameter, with a solid core from which Type I C–S–H fibres grow. Sometimes fibres and rods resembling "AFt" growth are incorporated in the structure. Fig. 11 shows an isolated spherulite in twelve-day paste, with a solid core from which C–S–H and "AFt" fibres radiate. Fig. 12 shows spherulites sectioned in two-dimensions during fracture of seven-day old paste, with some associated fibrous "AFt" growth.

Hadley grain formation, accompanied by the expulsion of solution into surrounding space, may provide a possible explanation for the formation of the small spherulites. Their morphology and distribution [2] is reminiscent of nucleation and growth so as to fill space [13]. Indeed, the fact that the proportion of Type III C–S–H in cement appears to be greater than that observed in C_3S [14] may be associated with these

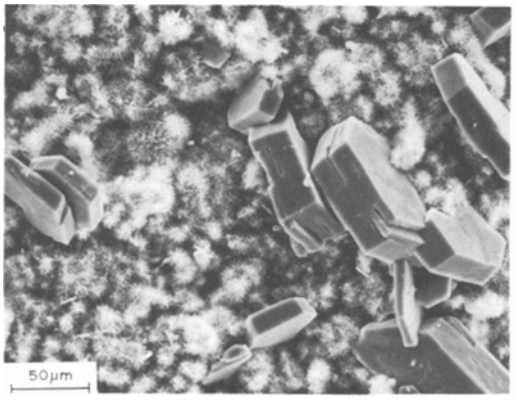

Figure 9 Interparticle fracture of three-day cement paste.

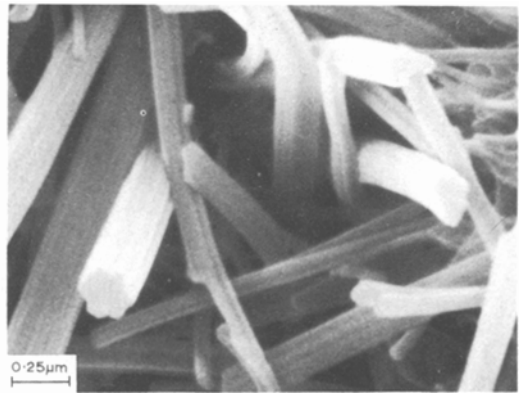

Figure 10 "AFt" fibres in three-day cement paste.

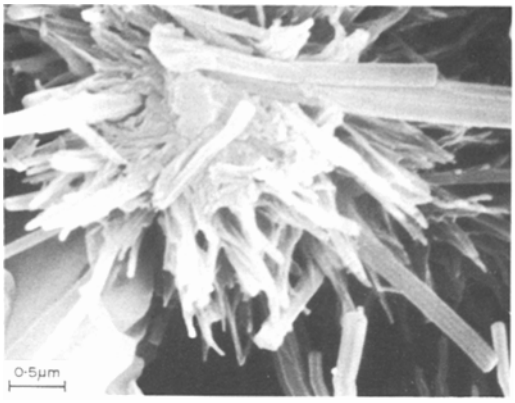

Figure 11 C–S–H and "AFt" growth from the solid core of a spherulite in twelve-day cement paste.

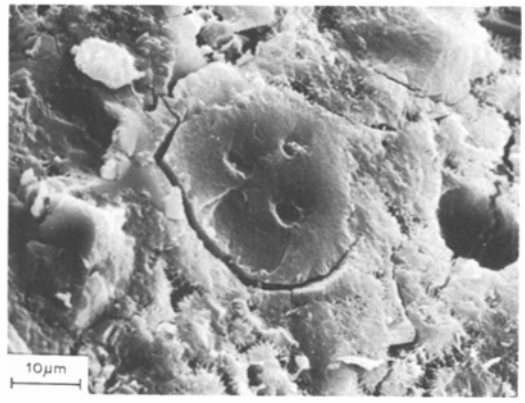

Figure 13 Transparticle fracture of 20-day cement paste.

spherulites packing space between grains. However, further study is required to determine their growth characteristics and their relationship with Hadley grain formation.

In young pastes interparticle fracture occurs through the developing gel and around the rigid inclusions of CH [15, 16]. However, after seven days hydration [2] the extent of transparticle fracture is significant. Fig. 13, after 20 days, shows a fairly flat crack path through regions of dense C–S–H and unhydrated clinker, and less dense structure which appears to comprise small spherulites in open space. There is also evidence that many spherulites are losing their identity as they intergrow, and fibrous material interlocks or becomes engulfed by CH [11, 17], as shown in the micrograph of Fig. 14.

As cement paste matures the CH crystals form a massive structure so that an interparticle crack path becomes too tortuous, and the energy requirement exceeds that for CH cleavage. Alternatively, as the C–S–H becomes more dense and homogeneous, and develops strength and rigidity, so the energy requirement for fracture becomes similar to that for CH cleavage. Fig. 15 illustrates predominantly transparticle fracture in an eight-month cement paste. Failure has occurred via a relatively straight path through extensive regions of CH and dense massive C–S–H. The regions of CH are identified by the stepped structure produced by cleavage. The C–S–H displays the fine equant granularity typical of Type III and forms a significant proportion of the total hydration product. Fibres and platelets typical of "AFt" and "AFm" growth, respectively, were observed in isolated porosity of the eight-month microstructure, and low density regions were observed in which the fine-particle gel structure had retained its initial fibrous morphology.

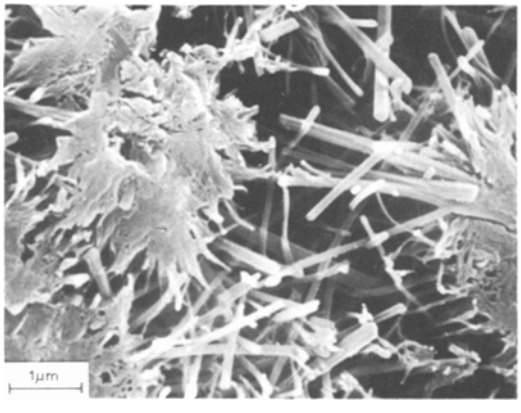

Figure 12 Spherulites sectioned in two-dimensions during fracture of seven-day cement paste.

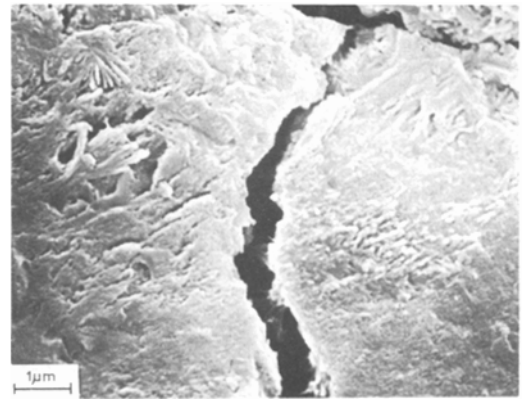

Figure 14 Fine C–S–H structure losing its identity to form a massive structure in seven-day cement paste.

3.3.4. Large spherical pores

Whilst C–S–H may be important in determining fracture characteristics, porosity and interlayer water are the more significant factors [18, 19], the latter influencing the creep and crack growth behaviour in particular. The spherical pore observed in Fig. 15 is probably a mixing pore caused by entrapped air, which became partially filled by subsequent CH growth. This type of pore was commonly observed, often at much larger sizes. An example is shown in the micrograph of three-day paste (Fig. 16) in which fracture has occurred between the developing C–S–H and CH precipitated at the pore surface. The extent to which the size and shape of this type of pore is modified during hydration will be dependent on the initial size which, in turn, will be determined by mixing and casting procedures.

Recently, Birchall *et al.* [4] demonstrated the influence of these macropores as strength-controlling Griffith flaws in seven-day ordinary Portland cement paste of low water/cement ratio. By removing such large defects they have produced material with much improved fracture properties.

4. Conclusions

(a) Scanning electron microscopy used in conjunction with energy dispersive analysis enables a comprehensive study of morphological development during the hydration of Portland cement paste, and provides a qualitative assessment of the chemical nature of the constituents. The basic appearance of the microstructure, after hydration for a day, is one of C–S–H fibres (mainly Type I) radiating out from the surface of calcium silicate grains, with CH crystals and minor phases forming in the capillary porosity. As the paste matures the microstructure develops into one of massive CH dispersed in predominantly Type III C–S–H.

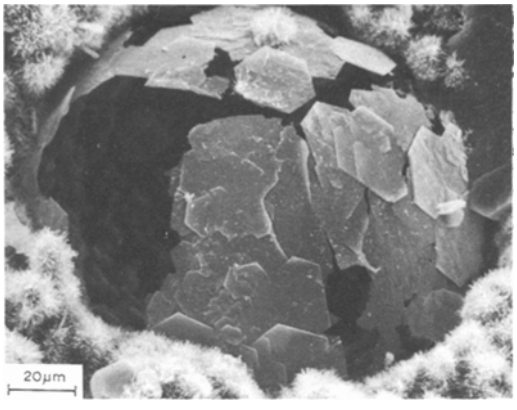

Figure 15 Transparticle fracture of eight-month cement paste revealing cleavage of massive CH dispersed in predominantly Type III C–S–H.

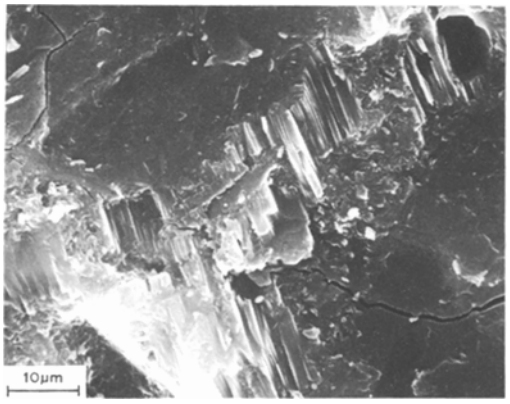

Figure 16 Large pore on the fracture surface of three-day cement paste, partly covered with CH.

(b) In yound cement paste interparticle fracture predominates, the crack passing through porous regions of C–S–H and avoiding regions where CH has precipitated to form rigid inclusions. In mature paste the crack path is less tortuous and transparticle fracture predominates. Failure occurs through extensive deposits of CH and massive C–S–H along a relatively straight path.

(c) Hadley grains were a significant feature of the hydrated cement paste microstructure observed in this study (water/cement ratio = 0.5). Although the extent of hollow shell formation is difficult to assess, the fact that it occurs questions some aspects of accepted cement hydration models, and the assumption that inner-product develops in close contact with outer-product in all grains.

(d) A series of very small spherulites is observed on the fracture surface of young cement pastes. In mature paste most of the spherulites become obscured in massive structure, but some are observed in isolation in the less dense regions of the structure. Details of their growth characteristics have yet to be established.

Acknowledgements

The authors wish to thank Blue Circle for supplying the cement, JEOL (UK) for the use of the microscope, and the Marine Technology Directorate of SERC for financial support.

References

1. S. DIAMOND, "Hydraulic Cement Pastes – Their Structure and Properties" Conference Proceedings, University of Sheffield, April, 1976 (Cement and Concrete Association, Wexham Springs, Slough, 1976).
2. B. J. DALGLEISH, P. L. PRATT and R. I. MOSS, *Cem. Concr. Res.* **10** (1980) 665.
3. P. J. SEREDA, R. F. FELDMAN and V. S. RAMACHANDRAN, Proceedings of the 7th International Congress on Chemistry of Cement, Vol. 1, Principal Rep. VI-I (3-44) Editions, Paris, September, 1980 (Editions Septima, Paris, 1980).
4. J. D. BIRCHALL, A. J. HOWARD and K. KENDALL, *Nature* **289** (1981) 388.
5. B. J. DALGLEISH, A. GHOSE, H. M. JENNINGS and P. L. PRATT, Proceedings of the 11th International Conference on the Science of Ceramics, Vol. II, edited by R. Cartsson and S. Karlsson (Swedish Ceramic Society, Gottenburg, 1981).
6. J. F. YOUNG, *Cem. Conce. Res.* **2** (1972) 415.
7. D. D. DOUBLE, A. HELLAWELL and S. J. PERRY, *Proc. Roy. Soc.* **A359** (1978) 435.
8. H. M. JENNINGS and P. L. PRATT, Proceedings of the British Ceramic Society, Vol. 28, edited by D. Taylor and P. S. Rogers, (British Ceramic Society, Stoke-on-Trent, 1979) p. 179.
9. B. D. BARNES, S. DIAMOND and W. L. DOLCH, *Cem. Concr. Res.* 8 (1978) 263.
10. B. J. DALGLEISH and K. IBE, *ibid.* **11** (1981) 729.
11. B. J. DALGLEISH and K. IBE, *JEOL News*, **18E**, 1 (1980) 9.
12. H. M. JENNINGS and P. L. PRATT, *J. Mater. Sci.* **15** (1980) 250.
13. M. AVARMI, *J. Chem. Phys.* 7 (1939) 1103.
14. H. M. JENNINGS, B. J. DALGLEISH and P. L. PRATT, *J. Amer. Ceram. Soc.* **64** (10) (1981) 567.
15. R. B. ROBERTSON, "Electron Microscopy and Structure of Materials", edited by G. Thomas, R. M. Fulrath and R. M. Fisher (University of California Press, Berkeley, 1972) p. 1223.
16. R. L. BERGER, F. V. LAWRENCE and J. F. YOUNG, *Cem. Concr. Res.* **3** (1973) 497.
17. T. D. CIACH, J. E. GILLOT, E. G. SWENSON and P. J. SEREDA, *ibid.* **1** (1971) 13.
18. R. F. FELDMAN and J. J. BEAUDOIN, *ibid.* **3** (1973) 497.
19. T. S. NADEAU, S. MINDESS and J. M. HAY, *J. Amer. Ceram. Soc.* **57** (2) (1974) 51.

Received 25 September
and accepted 15 December 1981